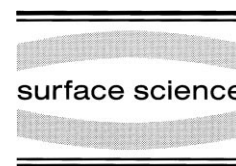




ELSEVIER

Surface Science 406 (1998) L597–L602



Surface Science Letters

Percolative growth of palladium ultrathin films deposited by plasma sputtering

Pascal Brault ^{a,*}, Anne-Lise Thomann ^a, Caroline Andreazza-Vignolle ^b

^a *Groupe de Recherches sur l'Energétique des Milieux Ionisés, UMR 6606 CNRS, Université d'Orléans, BP 6759, F-45067 Orleans Cedex 2, France*

^b *Centre de Recherches sur la Matière Divisée, UMR 6619 CNRS, Université d'Orléans, BP 6759, F-45067 Orleans Cedex 2, France*

Received 28 October 1997; accepted for publication 10 March 1998

Abstract

Palladium ultrathin films have been deposited by a plasma sputtering technique. In a first step, small particles (mean diameter $d < 3$ nm), homogeneously distributed on amorphous carbon membrane surfaces, are grown by surface diffusion of Pd atoms. Coalescence starts to form meandering compound clusters. Such Pd clusters, composing the islands, are still enlarging during the deposition. During the coalescence, a percolating network builds up with a measured percolation threshold around $p_c = 0.7$. The time evolutions of the mean size of the elementary and compound clusters are slightly modified when compared to vacuum deposition and theoretical predictions. © 1998 Elsevier Science B.V. All rights reserved.

Keywords: Amorphous surface; Atom–solid reaction; Carbon; Clusters; Diffusion and migration; Growth; Metallic films; Models of surface kinetics; Palladium; Scanning transmission electron microscopy; Surface defects

Metal deposition is of great interest in microelectronics [1–3], for preparation of catalysts [4–6], magnetic materials [7–9], gas sensors [10]. In this letter, we will emphasize the growth and ordering of palladium clusters on carbon membranes, due to its importance as a model catalyst [11–19].

The experimental setup is drawn in Fig. 1. Let us briefly summarize the main features. The Pd atom source is a helicoidal wire located between the substrate and the excitation antenna in a vacuum vessel that can be filled with a buffer gas (argon here). As the high frequency generator (100 MHz) is switched on, an argon plasma is

created. The Pd wire being negatively biased by a continuous bias generator, Ar ions are attracted and can sputter the wire. The Pd atoms emitted towards the substrate can thus be deposited. It is important to note that the substrate is also exposed to the Ar plasma. Thus the carbon surface is submitted to a low argon ion flux, with kinetic energy in the range 10–30 eV, during the deposition process [1,2]. The main interest in this process lies in the ability to induce surface heating and/or create surface defects which can act as nucleation sites. Thus, growth kinetics in such conditions deserve special attention.

The deposition rate R is measured by Rutherford backscattering spectrometry (RBS) using a 2 MeV He^+ particle beam extracted from a Van de Graaf

* Corresponding author. Fax: (+33) 238 417154; e-mail: pascal.brault@univ-orleans.fr

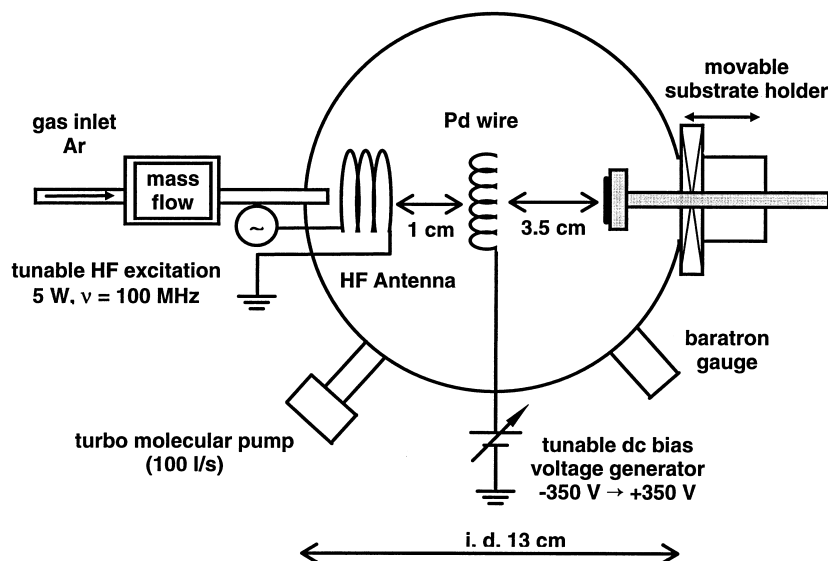


Fig. 1. Schematics of the experimental setup.

accelerator. High resolution transmission electron micrographs are obtained with a Philips CM 20 microscope (200 kV accelerating voltage) in order to study the size distribution, morphology and ordering of Pd clusters grown on amorphous carbon membranes.

Plasma deposition conditions were $P = 10^{-1}$ mbar, $V_b = -350$ V, P being the Ar pressure (the base pressure is 3×10^{-6} mbar) and V_b the Pd wire bias voltage. The resulting deposition rate as measured by RBS is $R = 6.3 \times 10^{13}$ at $\text{cm}^{-2} \text{s}^{-1}$. The substrate temperature T_s is 300 K. The deposition time was varied between 1 and 15 min. Above 15 min deposition duration, the films become flat and completely cover the surface [20,21].

The corresponding Pd island distributions are shown in Fig. 2a–e. It appears that homogeneous growth occurs, where elementary clusters display a single size. Single sized Pd clusters (mean diameter $d = 3$ nm) are well dispersed on the surface at $t = 1$ min and $n_{\text{Pd}} = 3.8 \times 10^{15}$ at cm^{-2} (n_{Pd} = palladium atom density on the surface). At $t = 2$ min coalescence already begins with numerous clusters formed by two or three coagulated elementary clusters forming ramified compound clusters. At the same time, the diameter of isolated elemen-

tary clusters has increased to $d = 3.5$ nm. Compound clusters seem to form by sticking of elementary clusters without penetration, like sticking hard spheres can do. Such a structure, undistorted stuck hard spheres, is clearly distinguishable on TEM micrographs (Fig. 2b–2e). Moreover, when the deposition time is increased, the elementary clusters belonging to a compound cluster are individually enlarged with the same size of isolated elementary clusters. Thus, both mean sizes of elementary and compound clusters simultaneously increase. The number of elementary clusters forming the compound clusters increases with time, while isolated elementary clusters disappear. Continuous increase of the elementary clusters (either isolated or belonging to a compound cluster) is due to the constant Pd atom deposition. The late stage leads to a percolation network beyond $t = 10$ min (Fig. 2d–2e), for which the percolation threshold is measured to be $p_c = 0.7$. Particle statistics obtained from TEM micrographs are summarized in Table 1.

To improve our understanding of the plasma sputtering assisted Pd cluster growth, numerous theoretical ways are now available [22–36]. Especially, the relevant evolutions concern the

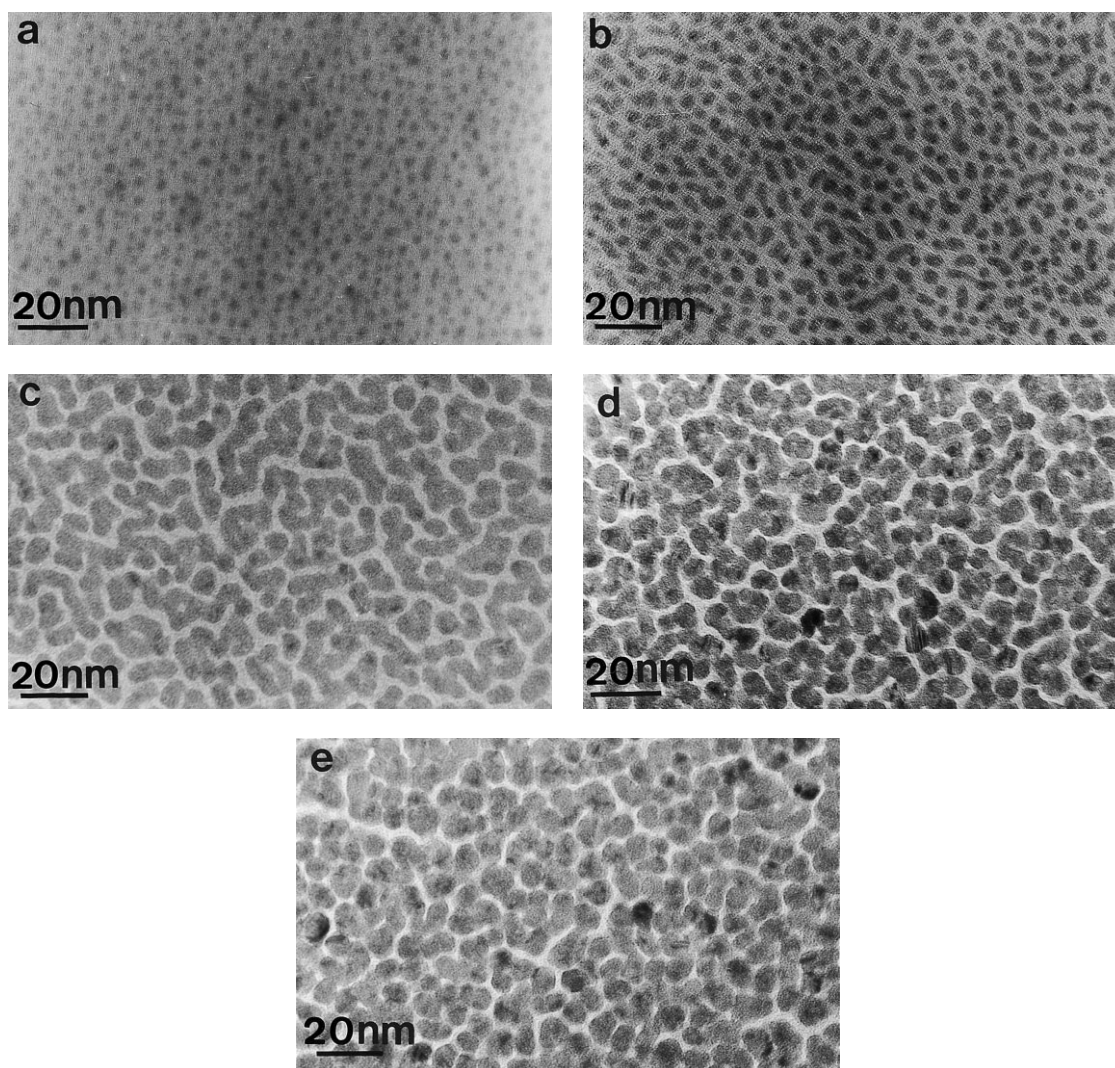


Fig. 2. TEM micrographs taken at different deposition times: (a) $t=1$ min, (b) $t=2$ min, (c) $t=5$ min, (d) $t=10$ min, (e) $t=15$ min.

Table 1
Particle statistics for deposition at $R=6.3 \times 10^{13}$ at $\text{cm}^{-2} \text{s}^{-1}$

t (min)	n_{Pd} (10^{15}cm^{-2})	Z_c (%)	N_c (10^{12}cm^{-2})	d (nm)	d_c (nm)
1	3.8	0.35	3.52	3	3
2	7.6	0.47	2.23	3.5	8.1
5	19	0.63	0.654	4.5	28.3
10	38	0.7	0.28	5	56.2
15	57	0.8	0.006	6	103

mean diameter $d(t)$ of the elementary clusters (either isolated or belonging to a compound cluster) and $d_c(t)$, the mean size of compound clusters $\{d_c(t) = [\sum_s N_s s^2 / \sum_s N_s s] d(t)$, s being the number of elementary clusters of the N_s compound clusters) [28,31] and the island densities $N_c = f(d_c)$. When looking at the evolution of the elementary cluster diameter d against t (Fig. 3), we find that $d \propto t^{1/4}$: that means that elementary clusters are growing via surface diffusion of the Pd atoms [25]. Scaling theories [23,31,35] indicate that $d \propto t^z$ and $d_c \propto t^{\alpha z}$ with $\alpha z = 1/(D_c - D_s)$ and $\alpha = D_c/(D_c - D_s)$, where D_c is the dimensionality of the cluster, $D_c = 3$, and D_s is the dimensionality of the surface ($D_s = 2$). This leads to $d \propto t^{1/3}$ and $d_c \propto t$. In our case, $z = 1/4$ instead of $1/3$, which is found in numerous experimental reports [22,23,37–39] (in Ref. [39] it is claimed that nucleation kinetics, for vapor deposition experiments, follow $t^{1/3}$). However, Beysens et al. [23] pointed out that an exponent $z = 1/4$ rather than $z = 1/3$ arises when temperature gradients are present in the substrate. Moreover, it was reported by Grant Elliot [40], in a study of Au deposition on mica, that a high density of nucleus can result in a slower cluster size growth.

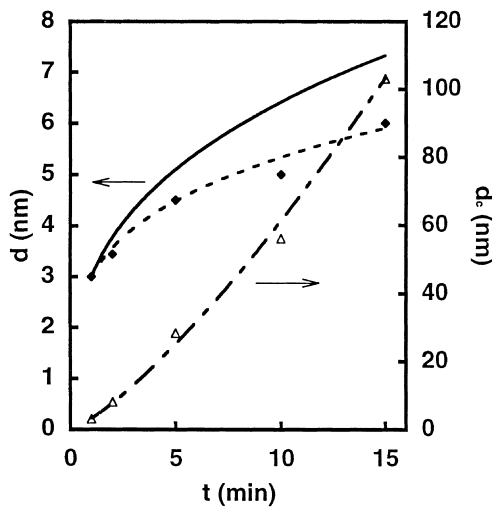


Fig. 3. Plots of the mean diameters d and d_c of the elementary (left vertical axis) and compound (right vertical axis) clusters against deposition time t . The solid line is the predicted $d \propto t^{1/3}$ law. The dashed line corresponds to the best fit: $d \propto t^{1/4}$. The dot-dash curve is the best fit $d_c \propto t^{1.28}$. Note that error bars are given by the size of the symbols.

Thus, because ion impingement can heat significantly the surface during deposition [1,2], it becomes possible to attribute the lowering of the dynamical exponent z to surface heating. We can also argue that the impinging ions create additional trapping surface sites, so if diffusing Pd atoms encounter such trapping sites they create new nucleation sites and cannot contribute to cluster size increase. This leads to a fast growth of the cluster density, and accordingly slows down the cluster size increase.

We can also observe that the cluster density N_c remains very high up to coverage $Z_c = 0.7$, i.e. $N_c = 0.28 \times 10^{12} \text{ cm}^{-2}$. It is currently observed and predicted that there exists a critical coverage, Z_0 , leading to the complete packing of the surface, i.e. N_c goes to zero. Such coverage is expected to range between $Z_0 = 0.5$ and 0.6 [22–24] for static coalescence. More precisely, in this case Z_c should obey the linear relation $Z_c = Z_0[1 - (N_c/N_0)]$ [22,24], where N_0 represents an initial maximum possible cluster density. Using the values reported in Table 1, we find that $Z_0 = 0.75$ and $N_0 = 6.2 \times 10^{12} \text{ cm}^{-2}$. Similar values were reported in previous measurements [37,38] dealing with vacuum vapor deposition. Indeed, it was reported that $Z_0 = 0.72$, $N_0 = 5 \times 10^{12} \text{ cm}^{-2}$ for Pd deposition on amorphous silica [37] and $Z_0 = 0.79$, $N_0 = 5.9 \times 10^{12} \text{ cm}^{-2}$ for Pd deposition on amorphous carbon. On the other hand, for Ag deposition on amorphous carbon [23] in conditions similar to Ref. [38], it was found that $Z_0 = 0.55$ in agreement with the Vincent prediction: $Z_0 = 0.5–0.6$. Metal deposition on CaF_2 [22] also provided a successful test of the Vincent prediction ($Z_0 = 0.55$). Thus, looking at the agreement between our Z_0 value and the previously reported ones, it is difficult to conclude whether the plasma has a visible effect on the coalescence process. In any case, it seems that departures from Vincent prediction would mean that coalescence is not purely static and that a dynamical step may exist in this process.

In Fig. 4 is plotted the island density N_c as a function of the mean compound cluster diameter d_c . The shape of this function is consistent with a dynamic coalescence occurring through cluster diffusion [25,36], which in turn is in agreement

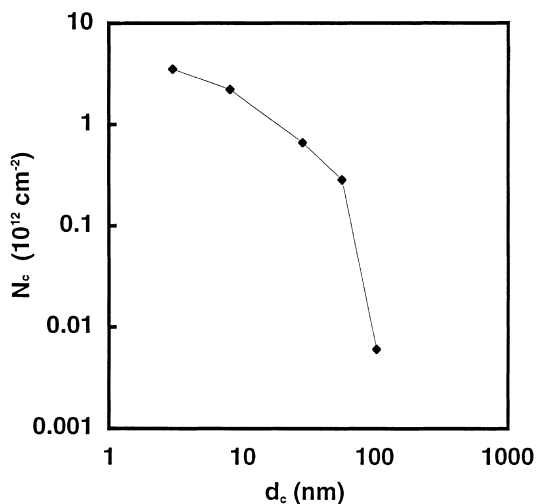


Fig. 4. Plot of the evolution of compound cluster densities N_c against mean diameter d_c . The curve is shown to guide the eye.

with the departure from the Vincent prediction $Z_0 = 0.5$ – 0.6 . For metal deposition on ionic crystals or amorphous substrates, it was clearly established that clusters containing several hundred to a few thousand atoms can move on a surface at room temperature [41–45]. Moreover, it was very recently demonstrated, using molecular dynamics calculations, that such large clusters can move freely on a surface even at room temperature as soon as the cluster is not commensurate with the substrate surface [43] and thus the cluster is no longer locked to the substrate. Such an effect is expected to depend on the size of the cluster. At the same time, Bardotti et al. observed that large (100 to 1000 atoms) gold and antimony clusters non-epitaxially oriented have very large diffusion coefficients. Such a counterintuitive result was interpreted by the role of substrate and cluster internal vibrations. Indeed, a random force is created as a result of these vibrational motions which leads to a Brownian-like motion of the cluster.

At last, in Fig. 3, the time evolution of d_c is plotted and well fitted by $d_c \propto t^{1.28}$. We have to note that, unfortunately, Refs. [37,38] were not concerned with the late stage of coalescence. Thus no exponent αz is available for further comparison. Only Beysens et al. performed such a complete

study, and they found that $\alpha z = 1$. But it remains difficult to establish whether in our case the departure from a linear growth is significant. We also note that if the dimensionality analysis described above is applied, starting from $z = 1/4$ should give $\alpha z = 0.75$ rather than 1. In this case, our exponent $\alpha z = 1.28$ becomes more significant. To clarify the discussion on dynamic coalescence, it seems useful to emphasize the following analysis. Exponents in the range 0.75–1 are found in experiments dealing with droplet growth, and are attributed to droplet coalescence [23,35] (cluster size of the same order as ours), but it is slightly different from theoretical prediction $\alpha z = 1, 1.4$ (Refs. [35,36], respectively). $\alpha z = 1$ was obtained for droplet coalescence into a new larger droplet [25,35]. The latter case, $\alpha z = 1.4$, was obtained from Monte-Carlo calculations describing cluster–cluster aggregation along straight trajectories on a surface [36]. On the other hand, Jensen et al. [34] found in simulations that the mean cluster size d_c should grow exponentially with time when coalescence occurs as cluster diffusion takes place. It was also suggested that such a regime will be a criterion for evidencing cluster coalescence into ramified compound clusters. In our case, we do not find such exponential growth, but a power law closer to Vicsek's prediction [36].

Because there exist large discrepancies between various theoretical and experimental works on coalescence, it remains difficult to conclude unambiguously that our results lead to a pure dynamical or static coalescence. However, regarding all the results reported in the literature compared to ours, we have the feeling that even if dynamical coalescence is not clearly evidenced, some dynamical effects exist in this process.

In conclusion, before the coalescence, elementary clusters are single sized and homogeneously distributed on the surface and grow via atom diffusion and further sticking. The compound clusters are growing and form larger meandering clusters until percolation is reached. Both growth rates of elementary and compound clusters are deduced, leading to dynamical exponents $z = 1/4$, $\alpha z = 1.28$ and critical coverage $Z_0 = 0.75$. Such characteristics of the present growth process are thought to be partly due to the role of impinging ions during the deposition.

Acknowledgements

The reviewer is gratefully acknowledged for illuminating comments.

References

- [1] S.M. Rossnagel, J.J. Cuomo, W.D. Westwood, Handbook of Plasma Processing Technology, Noyes Publications, Park Ridge, NJ, 1990.
- [2] B. Chapman, Glow Discharge Processes, Wiley, New York, 1980.
- [3] H. Von Kaenel, Mater. Sci. Rep. 6 (1991) 53.
- [4] S. Haukka, E.-L. Lakomaa, T. Suntola, Appl. Surf. Sci. 75 (1994) 220.
- [5] P. Hermann, B. Tardy, D. Simon, J.M. Guinier, B. Bigot, J.C. Bertolini, Surf. Sci. 307–309 (1994) 422.
- [6] J.C. Bertolini, P. Miegge, P. Hermann, J.L. Rousset, B. Tardy, Surf. Sci. 331–333 (1995) 651.
- [7] P. Ziemann, E. Kay, J. Vac. Sci. Technol. 21 (1982) 828.
- [8] P. Ziemann, E. Kay, J. Vac. Sci. Technol. A1 (1983) 512.
- [9] Y. Otanai, H. Miyajima, M. Yamaguchi, Y. Nozaki, A.J. Fagan, J.M.D. Coey, J. Magn. Magn. Mater. 135 (1994) 293.
- [10] G.E. Poirier, R.E. Cavicchi, S. Semancik, J. Vac. Sci. Technol. A12 (1994) 2149.
- [11] C. Argile, G.E. Rhead, Surf. Sci. Rep. 10 (1989) 277.
- [12] L. Porte, M. Phaner, C. Noupa, B. Tardy, J.C. Bertolini, Ultramicroscopy 42–44 (1992) 1355.
- [13] B. Tardy, C. Noupa, C. Leclercq, J.C. Bertolini, A. Hoareau, M. Treilleux, J.P. Faure, G. Nihoul, J. Catal. 129 (1991) 1.
- [14] C. Noupa, J.L. Rousset, B. Tardy, J.C. Bertolini, Catal. Lett. 22 (1993) 197.
- [15] A. Humbert, M. Dayez, S. Granjeaud, P. Ricci, C. Chapon, C.R. Henry, J. Vac. Sci. Technol. B9 (1991) 804.
- [16] I. Kojima, M. Kurahashi, J. Vac. Sci. Technol. B12 (1994) 1780.
- [17] A.A. Schmidt, H. Eggers, K. Erwig, R. Anton, Surf. Sci. 349 (1996) 306.
- [18] A.A. Schmidt, R. Anton, Surf. Sci. 322 (1995) 307.
- [19] M. Kuwahara, S. Ogawa, S. Ichikawa, Surf. Sci. 344 (1995) L1259.
- [20] A.L. Thomann, P. Brault, C. Laure, B. Rousseau, H. Estrade-Szwarckopf, C. Andreazza-Vignolle, P. Andreazza, A. Naudon, Surf. Coat. Technol. 98 (1998) 1228.
- [21] C. Laure, P. Brault, Plasma Sources Sci. Technol. 5 (1996) 510.
- [22] K.R. Heim, S.T. Coyle, G.G. Hembree, J.A. Venables, M.R. Scheinfein, J. Appl. Phys. 80 (1996) 1161.
- [23] D. Beysens, C.M. Knobler, H. Schaffar, Phys. Rev. B 41 (1990) 9814.
- [24] R. Vincent, Proc. Roy. Soc. London 321 (1971) 53.
- [25] M. Zinke-Allmang, L.C. Feldmann, M.H. Grabow, Surf. Sci. Rep. 16 (1992) 377.
- [26] J.A. Venables, G.D.T. Spiller, M. Hanbücken, Rep. Progr. Phys. 47 (1984) 399.
- [27] J.A. Venables, Phys. Rev. B 36 (1987) 4153.
- [28] D. Stauffer, A. Aharony, Introduction to Percolation Theory, Taylor and Francis, London, revised 2nd ed., 1994.
- [29] P. Meakin, Progr. Solid State Chem. 20 (1990) 135.
- [30] P. Meakin, Phys. Rep. 235 (1993) 189.
- [31] F. Family, P. Meakin, Phys. Rev. A 40 (1989) 3836.
- [32] R. Botet, R. Jullien, Ann. Phys. Fr. 13 (1988) 153.
- [33] G.S. Bales, D.C. Chrzan, Phys. Rev. B 50 (1994) 6057.
- [34] P. Jensen, A.-L. Barabási, H. Larralde, S. Havlin, H.E. Stanley, Phys. Rev. B 50 (1994) 15316.
- [35] J.L. Viovy, D. Beysens, C.M. Knobler, Phys. Rev. A 37 (1988) 4965.
- [36] T. Vicsek, F. Family, in: F. Family, D.P. Landau (Eds.), Kinetics of Gelation and Aggregation, Elsevier Science, The Netherlands, 1994, pp. 111–115.
- [37] Y. Takasu, R. Unwin, B. Tesche, A.M. Bradshaw, M. Grunze, Surf. Sci. 77 (1978) 219.
- [38] J.F. Hamilton, P.C. Logel, Thin Solid Films 16 (1973) 49.
- [39] R.M. Lambert, G. Pacchioni (Eds.), Chemisorption and Reactivity on Supported Clusters and Thin Films, Kluwer Academic, Dordrecht, 1997, pp. 117–152.
- [40] A. Grant Elliot, J. Vac. Sci. Technol. 11 (1974) 826.
- [41] C. Chapon, C.R. Henry, Surf. Sci. 106 (1981) 152.
- [42] C.R. Henry, C. Chapon, B. Mutaftschiev, Thin Solid Films 46 (1977) 157.
- [43] J.P. Deltour, J.L. Barrat, P. Jensen, Phys. Rev. Lett. 78 (1997) 4597.
- [44] L. Bardotti, P. Jensen, A. Hoareau, M. Treilleux, B. Cabaud, Phys. Rev. Lett. 74 (1994) 4694.
- [45] L. Bardotti, P. Jensen, A. Hoareau, M. Treilleux, B. Cabaud, Surf. Sci. 367 (1996) 267.